Friction of Soft Gel in Dilute Polymer Solution

Miao Du,[†,§] Yasuyuki Maki,[†] Taiki Tominaga,[†] Hidemitsu Furukawa,[†] Jian Ping Gong,[*,†,‡] Yoshihito Osada,[†] and Qiang Zheng[§]

Graduate School of Science, Hokkaido University, Sapporo 060-0810, Japan; SORST, JST, Japan; and Department of Polymer Science and Engineering, Zhejiang University, P.R. China

Received January 25, 2007; Revised Manuscript Received March 19, 2007

ABSTRACT: We study the friction behaviors of poly(vinyl alcohol) (PVA) gel sliding against glass surface in *dilute* poly(ethylene oxide) (PEO) aqueous solution with various molecular weights, M_w, and concentrations. At low sliding velocity (10^{-5}, 10^{-4} m/s), distinct PEO polymer effects are observed: The frictional stress in PEO 2E4 ($M_w = 2 \times 10^4$ g/mol) solutions is lower than that in pure water, decreasing with the increase in PEO concentration and reaching a minimum at the crossover concentration, c^*. However, in higher molecular weight solution, PEO 4E6 ($M_w = 4 \times 10^6$ g/mol), this friction reduction effect is only observed for very dilute concentration ($0.01c^*$ solution), and the friction stress in higher concentration ($0.1c^*$, $0.3c^*$, and c^* solution) is higher than that in pure water, accompanied by the appearance of "plateau". At fast sliding velocity (10^{-2}, 10^{-1} m/s), all the friction curves in dilute PEO solution superpose with the curve in pure water, independent of M_w and concentration of PEO. These results indicate that in the low sliding velocity region, where adsorption of PVA gel on glass plays the dominant role in friction, PEO chain screens the adsorption of PVA chains to glass surface. In the fast sliding velocity region, PEO chain is either extensively stretched or forms a deplete layer on the glass surface by the high shear rate, so the liquid lubrication with a viscosity of $\eta \approx \eta_{water}$ prevails. The results also support the theoretical prediction that the effective concentration of PEO in the confined 2-dimentional space between gel and glass interface is enhanced for high molecular weight PEO.

I. Introduction

Biological surfaces display fascinating low friction properties.[1−10] For example, cartilages of animal joints have a friction coefficient in the range 0.001−0.03, remarkably low even for hydrodynamically lubricated journal bearings.[1,2] It is not well understood why the cartilage friction of the joints is so low even in such conditions as that the pressure between the bone surfaces reaches as high as 3−18 MPa, and the sliding velocity is never greater than a few cm/s.[1] Under such conditions, the lubricating liquid layer cannot be sustained between two solid surfaces, and the hydrodynamic lubrication does not work. Cartilage cells synthesize a complex extracelluar matrix (ECM); the weight bearing and lubrication properties of cartilage are associated primarily with this matrix and its high water content (ca. 75−80 wt %). The main macromolecular constituents of ECM are the proteoglycan, aggrecan, and the cross-linked network of collagen fibrils.[6,7]

These fascinating tribological properties of the biological systems originate from the soft and wet nature of tissues and organs. That is, the role of solvated polymer network existing in ECM as a *gel state* is critically important in the specific frictional behavior of the biological systems. In order to elucidate the general tribological features of solvated polymer matrix, the friction of various kinds of hydrogels has been investigated using triobometer or rheometer, and very rich and complex frictional behaviors are observed.[11−26] The frictional behavior of hydrogels is dependent on the chemical structure of the gels, surface properties of sliding substrates, and the measurement conditions. It is considered that the surface friction of gels on a smooth substrate can be divided into two categories, that is, adhesive gels and nonadhesive gels, determined by the combination of the gels and the opposing surfaces. For adhesive gels, friction is from two contributions: namely, surface adhesion and hydrated lubrication. The former is dominant at low sliding velocities, and the latter is dominant at high velocities.[12] Transition in friction mechanism occurs at the sliding velocity characterized by the mesh size and polymer chain relaxation time of the gel. This transition is usually observed by the S-shape of friction with the increase in sliding velocity.[17] For nonadhesive gels, the friction, showing a monotonic increase with the sliding velocity, is believed due to lubrication of water layer. The presence of nonadhesive dangling chains on gel surfaces dramatically reduces the friction, and the brush gels show the friction coefficient as low as 10^{-4}, which is comparable with that of an animal joint.[16] There are a number of works on friction of gels using the surface force balance technique; these results give more direct information on the interfacial molecular interaction that contribute to the gel friction.[27,28]

The friction events in a biological system mostly occur between soft and wet tissues intermediated by viscoelastic polymer fluids, such as synovial fluid or mucus.[10] For example, mucus adheres to many epithelial surfaces, where it serves as a diffusion barrier against contact with noxious substances (e.g., gastric acid and smoke) and as a lubricant to minimize shear stresses; such mucus coatings are particularly prominent on the epithelia of the respiratory, gastrointestinal, and genital tracts.

Table 1. c^* Estimated from the Intrinsic Viscosity, Viscosity η^* of c^* Solution Experimentally Measured at Zero Shear Rate, Polymer Coil Size R_F, and the Osmotic Pressure π^* at c^* of Two Kinds of PEO with Different Molecular Weight M_w[a]

sample	M_w (g/mol)	c^* (g/dL)	η^* (10^{-3} Pa·s)	R_F (nm)	π^* (Pa)
2E4	2×10^4	2.85	2.8	12.0	5.0×10^3
4E6	4×10^6	0.085	4.5	283.3	3.5×10^{-1}

[a] R_F and π^* are estimated from eqs 1 and 7, respectively.

* Corresponding author: Tel +81 11 706 2774; fax +81 11 706 2774; e-mail gong@sci.hokudai.ac.jp.
† Hokkaido University.
‡ SORST.
§ Zhejiang University.

10.1021/ma0702187 CCC: $37.00
Published on Web 05/17/2007

Table 2. D and c_i/c_2^* of (a) Two Kinds of PEO Solution at $c = c^*$, (b) PEO 2E4 Solution of Various Concentrations, (c) PEO 4E6 Solution of Various Concentrations[a]

(a) $c = c^*$			(b) PEO 2E4			(c) PEO 4E6		
PEO	D (nm)	c_i/c_2^*	c/c^*	D (nm)	c_i/c_2^*	c/c^*	D (nm)	c_i/c_2^*
2E4	9.7	1.1	1	9.7	1.1	1	7.5	6
4E6	7.5	6	0.3	5.7	0.43	0.3	4.8	2.3
			0.1	3.7	0.18	0.1	3.2	0.94
			0.01	1.5	0.028	0.03	2.0	0.36
						0.01	1.3	0.15

[a] D and c_i/c_2^* are estimated values from eqs 17 and 29, respectively. Normal pressure: 14 kPa, 20 °C.

Mucus is also an abundant and important component of saliva, giving it virtually unparalleled lubricating properties.[8−10]

In this paper, we study the effect of *nonadhesive* polymer solution on the friction of *an adhesive* gel on a glass substrate. For simplicity, physically cross-linked poly(vinyl alcohol) (PVA) and linear poly(ethylene oxide) (PEO) were chosen as the gel and the polymer, respectively. There is no specific interaction between these two neutral and hydrophilic polymers. The effect of PEO molecular weight, M_w, and concentration, c, in the *dilute* region on the frictional behavior of PVA gel is investigated. The paper consists of three parts. In the first part, we experimentally studied the viscosity of PEO solution with different M_w and c and the properties of PVA gel in these PEO solutions. In the second part, we theoretically discuss the state of PEO chains in the confined space of interface between PVA gel and glass and estimate the polymer layer thickness under the normal pressure. In the third part, we experimentally study the friction of PVA gel in dilute PEO solution with various M_w and c.

II. Experiments

Materials. PVA and PEO with different molecular weight were produced by Wako Pure Chemical Industries, Ltd., and used without further purification. The degree of polymerization for PVA is 2000. The molecular weight scope of three kinds of PEO are $(2 \pm 0.5) \times 10^4$, $(3-5) \times 10^5$, and $(3.5-4) \times 10^6$ g/mol, which are coded as PEO 2E4, PEO 5E5, and PEO 4E6, respectively. Dimethyl sulfoxide (DMSO) was provided by Junsei Chemical Co., Ltd., and used as solvent without further purification.

Gel Preparation. Physically cross-linked PVA gel was prepared by a freezing (−40 °C) and thawing (25 °C) method, from a prescribed PVA aqueous solution (∼10 wt % PVA, DMSO:H_2O = 67.5:22.5 w/w).[29] Solutions were prepared by heating a mixture of PVA in the aqueous medium for 1 h at ∼90 °C. After the heating step, the PVA solutions were placed in a dryer connecting with a vacuum pump to facilitate the release of air bubbles. When all air bubbles were removed, the solutions were cast between glass plates and quenched for 24 h at −40 °C. Following the quenching period, hydrogel sheets (∼3 mm thick) were allowed to warm to room temperature and then submerged in copious distilled water at least 1 week to extract DMSO. After removing DMSO, the PVA gel was put into an excess of PEO aqueous solution of prescribed c and M_w for at least 1 week to obtain equilibrium.

Measurements. The viscosity of PEO solution was performed using a commercially available rheometer (3ARES-17A) with a pair of parallel plates of 50 mm diameter at 20 °C, covering a shear rate range from 10^{-2} to 10^3 s^{-1}. The gap distance between the plates was 0.5−1.0 mm.

The compressive modulus, E, of a gel was measured by using tensile-compressive tester (TENSILON, ORIENTEC., Co.) at 20 °C. The cylindrical gel sample of 10 mm diameter and 3 mm thickness was set on the lower plate and compressed by the upper plate, which was connected to a load cell at a velocity of 10% thickness/min. Since the gels used in this study were easily deformed, Hencky's strains (ϵ_h) and stresses (σ_h) were calculated, where ϵ_h and σ_h are the normal strain and stress, respectively. From the obtained relationship between ϵ_h and σ_h, we have calculated the modulus of compressive elasticity of each gel at a strain of less than 10%. The E of PVA gel swollen in pure water was 50 kPa. The mesh size, ξ, of PVA gel is ca. 5 nm as determined by dynamic light scattering, close to the value estimated from $E \approx kT/\xi^3$.

The friction force between PVA gel against a glass substrate in pure water or in PEO aqueous solution at 20 °C was performed using a rheometer (ARES, 2ARES-9A, Rheometric Scientific Inc.) that works in a constant compressive strain mode. The swollen PVA gel, ca. 3 mm in thickness, submerged in copious PEO aqueous solution, was cut into a disk shape of 15 mm diameter and then was glued on the upper surface of coaxial disk-shaped platen of rheometer with cyanoacrylate instant adhesive agent (Toa Gosei Co., Ltd.). The glass substrate, square shape of 25 mm in side, was glued onto the lower platen of rheometer. The separated gel−glass interface was immersed in pure water or PEO aqueous solution at a prescribed temperature and equilibrated for 30 min, and then the PVA gel was allowed to approach to glass surface at a velocity of 2 μm/s until the normal load increased to a prescribed value. Measurements were performed after the normal strain was applied for 10 min, whereupon an angular displacement was applied to the lower platen at a constant angular velocity (ω). Differing from the previous papers,[17,20] the angular velocity dependence at a certain experimental condition was studied by steady rate sweeping changes without separating the two rotating surfaces in the velocity change from lower to higher values. ω was increased stepwise from 10^{-3} to 10 rad/s for 40 s at each rotating velocity. The average torque T of last 20 s was adopted.

The frictional force, F, is calculated as $F = 4T/3R$, where T is the frictional torque recorded during measurement and R (=7.5 mm) is the radius of the apparent contact area. The average frictional shear stress, f, generated at the interface can be qualified as the friction force per unit area, $f = F/\pi R^2$. Although the sliding velocity varies along the radial direction in parallel plate geometry, we used the sliding velocity v at the outer side of disk-shape samples, $v = \omega R$.

III. Properties of PEO Aqueous Solution and PVA Gel

Solution Properties of PEO. Scaling theory describes each flexible linear polymer chain in an athermal solvent as a polymer coil, with a radius R_F in consideration of the excluded volume effect.[30]

$$R_F \cong aN^{3/5} \tag{1}$$

Here a is the Kuhn length and N is the number of Kuhn segments. The crossover concentration c^*, where the polymer coil start to contact, is

$$c^* \cong \frac{N}{{R_F}^3} \tag{2}$$

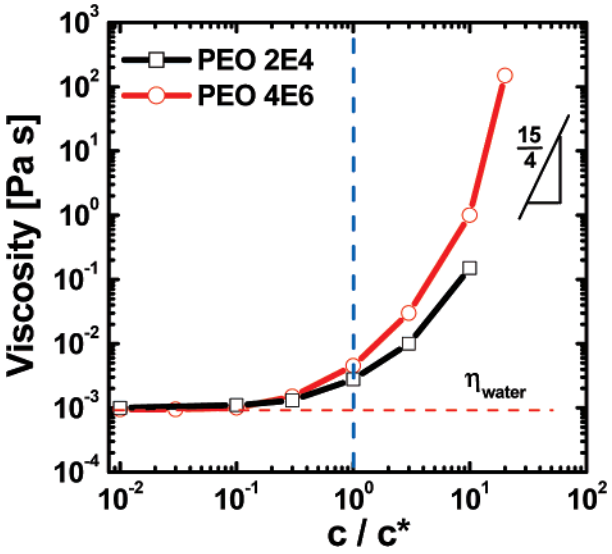

Figure 1. Relationship between viscosity at zero shear rate and the scaled concentration (c/c^*) for two kinds of PEO solutions with different molecular weight.

Substituting eq 1 for R_F to eq 2, we have

$$c^* \cong a^{-3}N^{-4/5} \tag{3}$$

The above equation says that a large N will bring on a diminutive c^* value. On the other hand, c^* is related to the intrinsic viscosity of polymer solution $[\eta]$ (dL/g) as

$$c^*[\eta] \approx 1 \tag{4}$$

while $[\eta]$ is related to the molecular weight M_w by the classic Mark−Houwink relation

$$[\eta] = KM_w^{\alpha} \tag{5}$$

where K and α are constants.[31] For PEO with diverse molecular weight, K and α are $(1.25-2.4) \times 10^{-4}$ and 0.73−0.78, respectively.[32] Using eqs 5 and 4, c^* of PEO with various molecular weight are calculated, shown in Table 1. It reveals that the real concentration of PEO 4E6 c^* solution is more than 30 times lower than that of PEO 2E4 due to its high molecular weight. Table 1 also shows the experimentally measured viscosity (η^*) of these c^* aqueous solution, which is very close to that of water, regardless of the huge differences in concentration and molecular weight.

Figure 1 depicts the measured viscosity η of PEO 2E4 and PEO 4E6 aqueous solution at different concentration, c, scaled by c^*. The η increases slightly with increase of c in the region $c < c^*$ but increases intensively when $c > c^*$. When $c/c^* > 10$, the viscosity is very close to the theoretical relation predicted for neutral polymer in the entangled region, $\eta \propto (c/c^*)^{15/4}$,[30,33] indicating the start of the concentrated region where polymers are entangled with each other.

It should be pointed that no shear thinning is observed for dilute PEO solution in the measurement region, where shear rate, $\dot{\gamma}$, is from 0.01 to 1000 s^{-1}. However, shear thinning appears in semidilute PEO solution when $\dot{\gamma}$ is very high. For example, shear thinning appears when $\dot{\gamma}$ is 10^2 s^{-1} for PEO 2E4 10c^* solution.

Effect of PEO Solution on PVA Gel. When a gel is immersed in a polymer solution that has no specific molecular interaction with each other, two effects are expected: (1) diffusion of soluble polymer chains into gel networks; (2) deswelling of gels by the osmotic pressure of polymer solution.

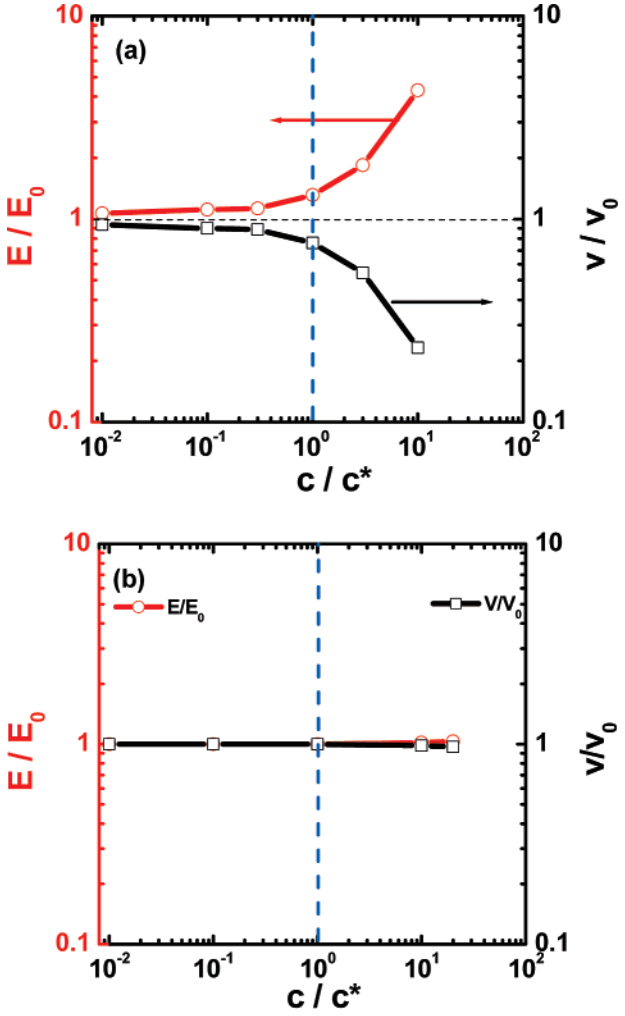

Figure 2. Dependence of relative compressive modulus (E/E_0) and relative swelling degree (V/V_0) of PVA gel on the scaled concentration (c/c^*) of PEO solution: (a) PEO 2E4; (b) PEO 4E6.

The first effect is related to the relative size of soluble polymer R_F to the gel network ξ. For the flexible vinyl polymer, the Kuhn length a and the number of the Kuhn segment N are approximately equal to the monomeric repeated length (=0.3 nm) and degree of polymerization (=M_w/44), respectively. Using $a = 0.3$ nm, R_F is estimated from eq 1 (Table 1). From Table 1, we know that R_F of PEO coils is 12.0 and 283.3 nm for PEO 2E4 and PEO 4E6, respectively, larger than the mesh size of PVA gel that is ca. 5 nm. So diffusion of PEO into PVA gel can be neglected.

Next, we consider the osmotic effect of PEO solutions on PVA gels using the results of scaling theory. In dilute polymer solution ($c/c^* \leq 1$), the osmotic pressure, π, is related to the polymer concentration, c, by[30]

$$\frac{\pi}{k_BT} \cong \frac{c}{N} + A_2c^2 \tag{6}$$

where $A_2 \cong R_F^3N^{-2} \cong a^3N^{-1/5}$ and k_B and T are the Boltzmann constant and absolute temperature, respectively. The above equation can be expressed in terms of c^*

$$\frac{\pi a^3}{k_BT} \cong N^{-9/5}\left[\frac{c}{c^*} + \left(\frac{c}{c^*}\right)^2\right] \quad (c/c^* \leq 1) \tag{7}$$

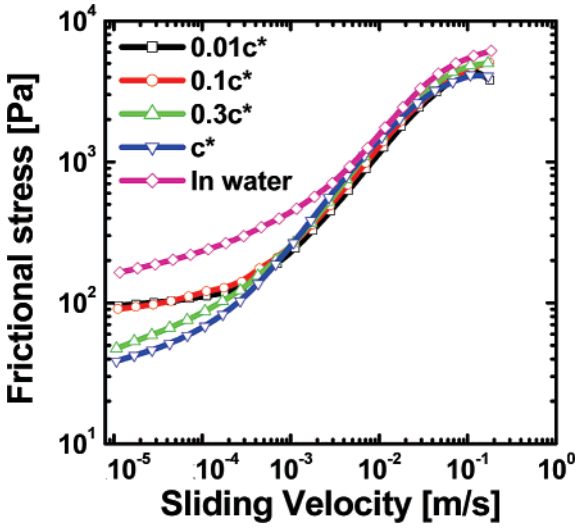

Figure 3. Sliding velocity dependence of the frictional stress for PVA gel sliding against a piece of glass surface in dilute PEO 2E4 solution with different concentration. Sample thickness: ~3 mm. Normal pressure: 14 kPa.

or in terms of osmotic pressure of solution at c^*, $\pi^* \cong k_BT/a^3N^{9/5}$.

$$\pi \cong \pi^*\left[\frac{c}{c^*} + \left(\frac{c}{c^*}\right)^2\right] \quad (c/c^* \le 1) \tag{7'}$$

In semidilute solution ($c/c^* \gg 1$), however, the osmotic pressure does not depend on N, and it scales with the polymer concentration as $\pi \propto c^{9/4}$.[30] We can also express the osmotic pressure in terms of c/c^* using the relation $c^* \propto N^{-4/5}$

$$\frac{\pi a^3}{k_BT} \cong N^{-9/5}(c/c^*)^{9/4} \quad (c/c^* \ge 1) \tag{8}$$

So the osmotic pressure both in the dilute solution and in the semidilute solution scales as $N^{-9/5}$ for the same c/c^*. For example, the osmotic pressure at c^* for PEO 2E4 and PEO 4E6 are 5×10^3 and 0.35 Pa, respectively. The former is comparable with the compressive modulus (50 kPa) of gel in pure water, and will deswell the gel, while the latter has a negligible effect on gel.

The molecular weight effect on the osmotic pressure is clearly observed in the swelling degree change of PVA gels in the PEO solutions. Figure 2 depicts the experimentally determined relation between the swelling degree (V/V_0) or compressive modulus (E/E_0) of PVA gel and the concentration (c/c^*) of PEO solution for PEO 2E4 and PEO 4E6. Here, V and V_0 are volumes and E and E_0 are compressive modulus of PVA gel in PEO solution and in pure water, respectively. The PVA gel shrinks slightly, and E/E_0 is close to unit in the region of $c < c^*$ in PEO 2E4 solution (Figure 2a). However, the gel shrinks dramatically and shows a high E in the $c/c^* > 1$ region, whereas in PEO 4E6 solution, PVA gels shows no change in volume and elasticity in both dilute and semidilute regions (Figure 2b).

From the above results, we know that the properties of dilute polymer solution differ greatly from the semidilute polymer (Figure 1) as well as the properties of PVA gel (Figure 2a). In the following section, the friction of PVA gels in dilute PEO solution, where the solution viscosity is close to water and gel modulus does not change, would be investigated. The friction behavior of PVA gels in semidilute and concentrated polymer solution will be reported in a separate paper.

IV. Theoretical Analysis of Polymer Solution Confined between Parallel Surfaces

We consider how the polymer in bulk dilute region ($c < c^*$, liquid has a viscosity close to water) is confined between two *nonadhesive* and *rigid* surfaces. When a disk-shaped rigid surface of radius R is allowed to approach to another hard surface in a liquid of viscosity η from a distance $h \ll R$ at a velocity dh/dt[9]

$$\frac{dh}{dt} = -\frac{2h^3P}{3\eta R^2} \tag{9}$$

For a constant velocity, $v_N = dh/dt$, the normal stress P changes as

$$P = \frac{3\eta R^2 v_N}{2h^3} \tag{10}$$

Equation 10 only holds when $h(t) \gg R_F$. When $h(t) \sim R_F$, the mobility of the confined polymer chains decreases, and the polymer coil will not be squeezed from the gap together with the water with a viscosity close to that of water. Therefore, we can assume that the thickness change at $h \le R_F$ is dominated by permeation of solvent through the polymer coil in a time scale we are interested. Here, we are not interested in the problem how the thickness of the gap will change with time in the $h \le R_F$ region, but the problem of a polymer chain of size R_F confined in a thin slit at a certain time.

We assume that the distance between the plates D is much smaller than the size of a polymer coil R_F but much larger than the effective monomer size a, that is, $a \ll D \ll R_F$. We derive the relation between the pressure P on the plates and D. The monomeric concentration in the layer of which the thickness is R_F equals the concentration of the bulk solution c

$$c \cong \frac{n_pN}{R_FA} \tag{11}$$

where A is the area of the plates and n_p is the number of the polymer chains in the slit. Here, we suppose that n_p does not change with the slit distance by two reasons: (1) the effective viscosity at $D \ll R_F$ increases, and the diffusion of the polymer chain is neglected in the time scale we interested; (2) ends of some polymer chains could be entangled with the network and a layer of polymer chains "grafted" onto the gel may be formed. So, the concentration c_i increases as the layer is compressed by the confinement.

$$c_i \cong \frac{n_pN}{DA} \cong \frac{R_F}{D}c \cong N^{3/5}\left(\frac{a}{D}\right)c \tag{12}$$

The normal pressure applied to the plates, P, is balanced by the osmotic pressure inside the slit π_i, $P = \pi_i$. In the confined slit of $D \ll R_F$[30]

$$\pi_i/k_BT \cong \frac{c_i}{N} + \frac{5}{3}c_i\left(\frac{a}{D}\right)^{5/3} \tag{13}$$

Here, the second term is due to the confinement of the polymer chain in the slit. From $P = \pi_i$ and eq 13

$$P/k_BT \cong \frac{c_i}{N} + \frac{5}{3}c_i\left(\frac{a}{D}\right)^{5/3}$$
$$\cong \frac{c}{N}\left[\frac{aN^{3/5}}{D}\right] + \frac{5}{3}N^{3/5}c\left(\frac{a}{D}\right)^{8/3} \quad (14)$$

Equation 14 can be written as

$$P \cong \pi\left[\frac{R_F}{D} + \frac{5}{3}\left(\frac{R_F}{D}\right)^{8/3}\right] \quad (15)$$

Here $\pi = ck_BT/N$ is the osmotic pressure of the outside solution. When $P/\pi \gg 1$, $D \ll R_F$, the second term of eq 15 is predominant, that is

$$\frac{P}{\pi} \cong \frac{5}{3}\left(\frac{R_F}{D}\right)^{8/3} = \frac{5}{3}N^{8/5}\left(\frac{a}{D}\right)^{8/3} \quad (16)$$

Equation 16 can be expressed in terms of c^*

$$P/k_BT \cong \frac{5}{3}\frac{1}{a^3N^{1/5}}\left(\frac{c}{c^*}\right)\left(\frac{a}{D}\right)^{8/3} \quad (17)$$

At the same c/c^* concentration and P, D is only weakly ($D \propto N^{-3/40}$) dependent on N. The order of D under $P = 14$ kPa for various dilute PEO solutions is estimated from eq 17, using parameters $a = 0.3$ nm and $k_BT = 4 \times 10^{-21}$J ($T = 293$ K). The results are shown in Table 2.

Next, we discuss the overlap concentration in the two-dimensional confined space, using the scaling theory.[30] When the concentration c_i inside the slit is described as eq 11, the confined chains are forced to overlap at a lower concentration than that in the bulk solution. The ordinary overlap threshold c^* in three-dimensional space is given as

$$c^* \cong \frac{N}{{R_F}^3} \sim \frac{N}{a^3N^{3\nu_3}} = \frac{N^{-4/5}}{a^3} \quad (18)$$

where ν_3 is an exponent on 3-dimensional space obtained from Flory exponent ν_d for d-dimensional space:[30]

$$\nu_d = \frac{3}{d+2} \quad (19)$$

The concentration at which the polymer chains inside the slit start to overlap, c_2^*, is written as

$$c_2^* \sim \frac{N}{D{R_2}^2} \quad (20)$$

where R_2 is the lateral size of a confined chain. The polymer confined between the surfaces is assumed to consist of blobs which are each D in size, and the chain of blobs is regarded as a self-avoiding chain on 2-dimensional space. The lateral size R is given as[30]

$$R_2 \sim D\left(\frac{N}{g}\right)^{\nu_2} \quad (21)$$

where g is number of monomers contained in a blob, and g is related to D as

$$D \sim ag^{\nu_3} \quad (22)$$

Substituting eqs 21 and 22 into eq 20, we obtain

$$c_2^* \sim \frac{N}{D^3(N/g)^{2\nu_2}} = \frac{N^{1-2\nu_2}}{D^3g^{-2\nu_2}} \sim \frac{N^{1-2\nu_2}}{D^3(D/a)^{-2\nu_2/\nu_3}}$$
$$= \frac{N^{-1/2}}{D^3(D/a)^{-5/2}} \quad (23)$$

Comparing eq 18 with eq 23, the relationship

$$\frac{c_2^*}{c^*} \sim N^{3/10}\left(\frac{D}{a}\right)^{-1/2} \quad (24)$$

is obtained. From eqs 11 and 24

$$\frac{c_i/c_2^*}{c/c^*} = N^{3/10}\left(\frac{a}{D}\right)^{1/2} = \left(\frac{R_F}{D}\right)^{1/2} \quad (25)$$

is derived. In the condition $a < D < R_F$

$$\frac{c_i/c_2^*}{c/c^*} > 1 \quad (26)$$

Therefore

$$\frac{c_i}{c_2^*} > \frac{c}{c^*} \quad (27)$$

At $c = c^*$

$$\frac{c_i}{c_2^*} > 1 \quad (28)$$

The above inequation shows that the scaled polymer concentration in the confined space is always higher that the bulk concentration and that the PEO chains start to overlap with each other in the confined space even if the bulk concentration is in c^* solution.

In order to see the effect of P, we combine eq 25 with eq 17 and express the relation in terms of c^* and the osmotic pressure of polymer solution at c^* and π^*:

$$c_i/c_2^* \cong \left(\frac{3Pa^3}{5k_BT}\right)^{3/16}N^{27/80}\left(\frac{c}{c^*}\right)^{13/16} = \left(\frac{3P}{5\pi^*}\right)^{3/16}\left(\frac{c}{c^*}\right)^{13/16} \quad (29)$$

Equation 29 indicates that the 2-D confinement effect on the polymer chain overlapping increases with the molecular weight, scaled as $c_i/c_2^* \propto N^{27/80}$. The equation also indicates that the 2-D confinement effect becomes important only when $P \gg \pi^*$.

Table 2a gives estimated values of D and c_i/c_2^* at $c/c^* = 1$ under P of 14 kPa. It can be seen that for PEO with high M_w, such as PEO 4E6, $P \gg \pi^* \approx 0.35$ Pa and $c_i/c_2^* = 6$, revealing that entanglement exists in the confined space even though $c/c^* = 1$. However, for PEO with low M_w, such as PEO 2E4, $P \approx \pi^* = 5 \times 10^3$ Pa and c_i/c_2^* at $c/c^* = 1$ is merely 1.1, showing that almost no entanglement exists in the slit. This result also indicates that PEO coils with low M_w in the confined space, i.e., PEO 2E4 at present, are difficult to deform. However, PEO coils with high M_w, such as PEO 4E6, are easy to be compressed and behave like a soft coil. These dissimilarities will give a striking difference in their rheological behavior and therefore result in different friction of PVA gel sliding against glass surface.

It should be pointed out that in the present system, instead of two rigid surfaces, the PEO is entrapped between the rigid

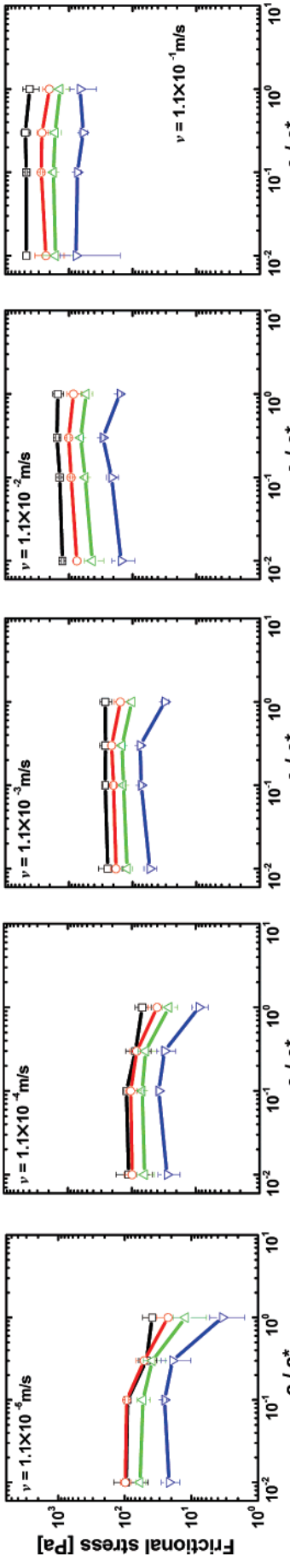

Figure 4. Concentration dependence at different sliding velocity for PVA gel friction in PEO 2E4 aqueous solution. Normal pressure: (□) 14, (○) 8.4, (△) 5.6, and (▽) 2.8 kPa.

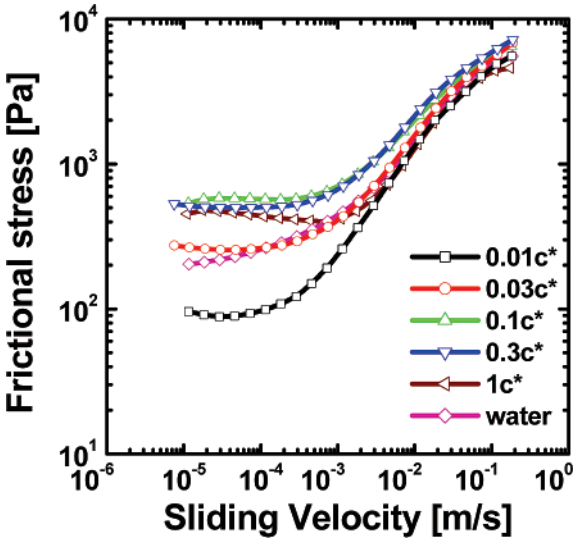

Figure 5. Sliding velocity dependence of the frictional stress for PVA gel sliding against a piece of glass surface in PEO 4E6 solution with different concentration. Sample thickness: ~3 mm. Normal pressure: 14 kPa.

glass surface and the soft gel surface with a compressive elasticity E of 50 kPa. For PEO 2E4, $\pi^* = 5 \times 10^3$ Pa is comparable to E, so the D in reality might be larger due to the deformation of gel, while for PEO 4E6, $\pi^* \ll E$, and the softness of the PVA gel can be neglected.

In the following section, the friction behavior of PVA gel against the glass surface in dilute PEO 2E4 and PEO 4E6 aqueous solution is discussed.

V. Friction of PVA Gel in Dilute PEO Solution

Experimental Results. *In PEO 2E4 Solution.* Figure 3 gives the friction behavior of PVA gel against glass surface in dilute PEO 2E4 solution under a normal pressure of 14 kPa. It is very interesting that the frictional stress in dilute PEO 2E4 solution is lower than that in pure water in low sliding velocity region, for instance, lower than 10^{-3} m/s, and the lowest friction appears in PEO 2E4 c^* solution, although the viscosity of the fluid slightly increases with the PEO concentration, as shown in Figure 1. However, with the increase of sliding velocity, the effect of PEO on friction diminishes, and all the friction curves superpose with the friction curve in pure water at velocities higher than 10^{-2} m/s.

In Figure 4, frictional stress is plotted against the PEO concentration c/c^* under normal pressure P of 14, 8.4, 5.6, and 2.8 kPa for various sliding velocities. The figure clearly shows that the PEO 2E4 reduces the friction at the low velocity, and this friction reduction effect gradually disappears at high velocity for all the normal pressures studied. Furthermore, Figure 4 shows that the lower the normal pressure applied, the higher the velocity that this friction reduction effect can persist.

In PEO 4E6 Solution. As shown in Figure 5, similar to that in dilute PEO 2E4 solution, the largest difference with that in pure water appears at low sliding velocity region, and all the friction curves superpose at fast sliding region in dilute PEO 4E6 solution. However, the friction reducing effect only observed in very dilute 0.01c^* solution. The frictional stress in PEO 4E6 0.1c^*, 0.3c^*, and 1c^* solution are higher than that in pure water and shows a wide "plateau" in low sliding velocity region, different from those in dilute PEO 2E4 solution. In Figure 6, frictional stress is plot against the PEO concentration under normal pressure P of 14, 8.4, 5.6, and 2.8 kPa for various

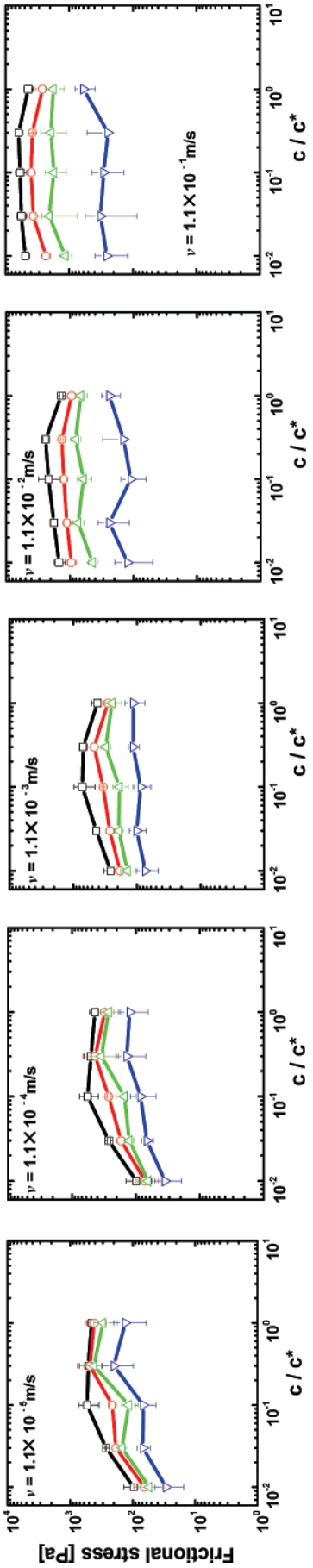

Figure 6. Concentration dependence at different sliding velocity for PVA gel friction in PEO 4E6 aqueous solution. Normal pressure: (□) 14, (○) 8.4, (△) 5.6, and (▽) 2.8 kPa.

sliding velocity. The figure shows that with the increase in c/c^* the frictional stress increases and reaches a maximum at a certain c/c^* value in the low velocity region, and this PEO concentration-dependent friction behavior gradually disappears with the increase in the sliding velocity. Furthermore, this PEO concentration-dependent behavior becomes less explicit under lower normal pressures.

Discussion. As described in the Introduction, for adhesive gels sliding on a smooth solid surface, friction is from two contributions: surface adhesion and hydrated lubrication. The former is dominant at low sliding velocities, and the latter is dominant at high velocities.[12] A transition in friction mechanism occurs at the sliding velocity characterized by the mesh size and polymer chain relaxation time of the gel. This transition is usually observed by the S-shape of friction with the increase in sliding velocity.[13,25] In Figure 3, PVA gel does not show a very clear transition in the stress−slip velocity curves that is characteristic for attractive interaction. This might attribute to the weak adhesion as well as the low modulus (50 kPa) of the sample used in the present study.

As discussed in the previous section, PEO coil layer exists in the space between PVA gel and glass surface, which prevents PVA blobs from being adsorbed on glass surface. Therefore, the adsorbing site number of PVA blobs in PEO solution will decrease with the increase in PEO concentration. The screening of PVA adsorption by PEO will reduce the friction at the low velocity region where PVA chain adsorption is dominant. When the PEO concentration increases up to c_2^*, a continuous PEO monolayer is formed, and the adsorption of PVA is completely screened. So the friction stress at this PEO concentration is given by lubrication of the PEO layer. We estimate the viscous shear resistance of the PEO 2E4 layer. At $v \sim 10^{-5}$ m/s, the shear rate $\dot{\gamma}_e = v/D \approx 10^3$ s^{-1}. So the low limit of shear resistance due to PEO monolayer is ~3 Pa, using the value of 3 mPa·s, determined from the viscosity of PEO 2E4 at c^* concentration. The observation of frictional stress ~40 Pa for PEO 2E4 c^* (Figure 3) is reasonably close to this estimation, considering that the actual viscosity at the interface might much higher than 3 mPa s.

As shown in Table 2a, $c_i/c_2^* \approx c/c^*$ for PEO 2E4 solution and $c_i/c_2^* \gg c/c^*$ for PEO 4E6 solution, at $P = 14$ kPa. This explains why we observe the lowest friction (the highest screening effect) at $c/c^* = 1$ for PEO 2E4 solution (Figure 3) while the friction reduction effect is only observed in PEO 4E6 0.01c^* solution (Figure 5). The higher friction in PEO 4E6 solution of $c/c^* > 0.1$ (Figure 5) than that in water is associated with the effect of $c_i/c_2^* \gg c/c^*$. In PEO 4E6 0.3c^* and c^* solution, c_i/c_2^* in the confined space is 2.3 and 6, respectively (Table 2c). So the adsorption of PVA to the glass substrate is completely screened in these solutions, and the friction is due to the viscoelastic effect of PEO entrapped between the gel and glass interface. The dramatically enhanced viscosity of the entangled PEO results in high friction. For PEO 4E6 0.03c^* and 0.1c^* solutions, we also observe a slightly higher friction force than that in water. This suggests that the actual c_i/c_2^* in the confined space might be much higher than the estimated value. Probably the actual confined space effect starts to work even at a gap thickness several times larger than R_F, especially for large molecular weight PEO.

Next, we discuss the velocity effect. The PEO shows pronounced effects on friction at low velocity, and the effect gradually disappears with the increase in the sliding velocity. The friction reduction effect sustains to a higher velocity under a lower normal pressure for PEO 2E4 (Figures 3 and 4), while

the friction enhancement effect continues to a higher velocity under a higher normal pressure for PEO4E6 (Figures 5 and 6). These velocity dependences of friction are considered due to (1) polymer stretching and (2) hydrodynamic water layer formation at high shear rate.

(1) Polymer Stretching. In a simple shear with shear rate $\dot{\gamma}$, a highly confined *unentangled* chain begins to be stretched away from its equilibrium value when the Weissenberg number $W_e = \dot{\gamma}\tau$ is in order unity, where τ is the relaxation time that related to the conformation change of the polymer. On account of extremely narrow thickness of slit between PVA gel and glass surface, the effective shear rate, $\dot{\gamma}_e$, exerts on PEO chain in the confined space is strikingly high. $\dot{\gamma}_e$ can roughly be estimated by v/D, at low velocity region. For example, at $v = 10^{-5}$ m/s, $\dot{\gamma}_e \sim 10^3$ s^{-1}. For $c_i/c_2^* < 1$, the longest relaxation time of the chain, τ, can be estimated using blob theory, $\tau \cong \eta D R_2^2/k_B T$, where $R_2 \cong N^{3/4} a (a/D)^{1/4}$ according to eqs 20 and 23. Therefore

$$W_e \cong \frac{\eta v}{k_B T} N^{3/2} a^2 (a/D)^{1/2} \qquad (30)$$

Equation 30 indicates that the Weissenberg number is strongly dependent on the molecular weight of the polymer ($W_e \propto N^{3/2}$) and not very sensitive to D ($W_e \propto D^{-1/2}$). For PEO 2E4, $W_e \approx 10^2 v$, as estimated from the known parameters. Therefore, the PEO 2E4 is stretched at $v > 10^{-2}$ m/s ($W_e > 1$), and this weakens the screening effect, and the frictional stress in PEO begins to approach to that in water, as shown in Figure 3. For PEO 4E6, $W_e \approx 10^5 v$. So, even at the lowest sliding velocity of 10^{-5} m/s, $W_e \sim 1$. This explains why we observe a weak velocity dependence of friction even at the lowest velocity in Figure 5 for PEO 4E6 0.01c^* solution.

For *entangled* polymers, the longest relaxation time is the reptation time, $\tau_{t(c)} \cong (N/g)^3 \tau_{blob}$, where $\tau_{blob} \cong \eta D^3/k_B T$. For the PEO 4E6 solution of $c_i/c_2^* > 1$, $\tau_{blob} \sim 10^{-7}$ s and $\tau_{t(c)} \sim 10$ s, as estimated from known parameters. So $\dot{\gamma}_c = \tau_{t(c)}^{-1} = 0.1$ s^{-1}. At $v = 10^{-5}$ m/s, $\dot{\gamma}_e \sim 10^3$ s^{-1}, much higher than the critical shear rate, indicating that shear thinning occurs for PEO 4E6 even from the lowest sliding velocity ($\sim 10^{-5}$ m/s). This explains why the frictional stress of PEO 4E6 of 0.1c^*, 0.3c^*, and 1c^* only increases slightly with the increase of velocity, and then it exhibits a plateau until 10^{-3} m/s, as shown in Figure 5. We can check this shear thinning effect by comparing the viscous resistance at the zero shear rate with the frictional stress. In PEO 4E6 c^* solution, $c_i/c_2^* \sim 6$, and from Figure 1, we know that the zero shear rate viscosity at $c/c^* = 6$ is $\sim$1 Pa·s. Thus, the shear stress due to the simple viscous resistance of PEO 4E6 at $v = 10^{-5}$ m/s (corresponding to a shear rate of 1.5×10^3 s^{-1}) should be $\sim$1500 Pa. This value is higher than the observed frictional stress of $\sim$600 Pa (Figure 5), confirming that the shear thinning occurs even at the lowest velocity of the present study. It is not clear why we observe a frictional stress even slightly higher than that at c^* for 0.1c^* and 0.3c^*.

(2) The Hydrodynamic Water Layer Formation. Essentially, if the polymer is nonadhesive to the wall, its depletion from the surface creates a layer of weak viscosity close to the wall when the shear rate is high.[34,35] This hydrodynamically induced depletion of polymer is observed as wall slip of PEO on the glass surface, recently by Degre et al. for the PEO aqueous solutions of high molecular weight (5×10^6 g/mol, similar as that of 4E6) at high concentration.[34] In the present study, the glass substrate is rotated and the gel is fixed, which gives Couette flow along the circuit direction. During rotation of the glass substrate, the PEO polymer will intend to migrate toward the gel surface to give a hydrodynamic deplete layer on the glass surface. So the friction in this velocity region is due to the hydrodynamic lubrication of liquid with a viscosity of $\eta \sim \eta_{water}$. This explains why the frictional stress at $v > 10^{-2}$ m/s completely superposes with that in pure water (Figures 3 and 5). At this velocity, if we assume the frictional stress originated from the hydrodynamic lubrication mechanism, we have the water layer thickness $h \sim 10$ nm at 0.01 m/s from Figures 3 and 5.

Finally, we discuss the normal pressure effect. In pure water, the frictional stress of PVA gel increases almost linearly (with

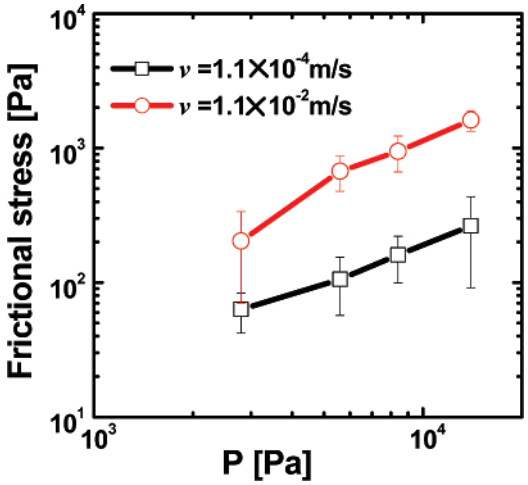

Figure 7. Experimental results of the dependence of the frictional stress on the pressure P for PVA gel sliding on the glass substrate in water under various sliding velocity.

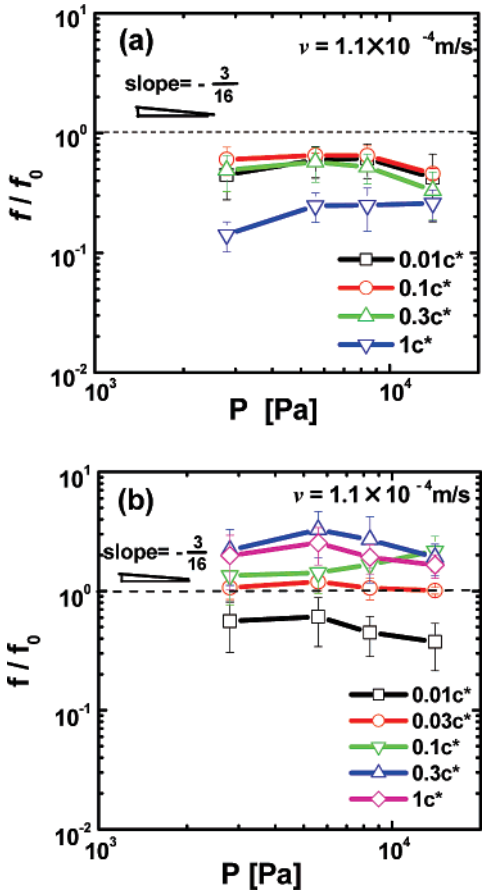

Figure 8. Ratios of frictional stress of PVA gel in PEO 2E4 (a) and PEO 4E6 (b) solution (f) to that in water (f_0) under various normal pressure P for various PEO concentration. Sliding velocity: 1.1×10^{-4} m/s.

a slope of one in the figure) with the increase of P, either at low velocity (10^{-4} m/s) or at high velocity (10^{-2} m/s) (Figure 7). This pressure dependence is stronger than that observed in the previous work using a tribometer.[13] This difference might originate from the different measurement conditions: The measurement performed by tribometer runs in the normal force constant mode, while the measurement using a rheometer in the present study runs in a normal strain constant mode. The normal pressure shown in Figure 7 corresponds to the value applied at the beginning of loading, which relaxes along with the time during measurement. A detailed study on the pressure dependence of frictional stress under a strain constant mode is beyond the scope of this work and should be studied in the future.

In PEO solution, eq 29 suggests that the effective polymer concentration at the confined space, c_i/c_2^*, weakly depends on the normal pressure P ($c_i/c_2^* \propto P^{3/16}$). This relation predicts that the screening effect of PEO on PVA friction is not sensitive to P, when $c_i/c_2^* < 1$. To testify this prediction, the ratios of frictional stress of PVA gel in PEO solution (f) to that in water (f_0) at low sliding velocity (10^{-4} m/s) are plotted against P for PEO 2E4 (Figure 8a) and 4E6 (Figure 8b). Here, the ratio of frictional stress (f/f_0) can be roughly regarded as a parameter to characterize the screening effect of PEO on adsorption of PVA chain to glass substrate. The frictional stress ratios (f/f_0) in both PEO 2E4 solution and PEO 4E6 solution show weak dependence on P, which indicates that the screening effect is not sensitive to normal pressure, and this is roughly in agreement with the theoretical prediction.

VI. Conclusions

When a water-swollen PVA gel is pressed on a glass surface in dilute ($c/c^* \leq 1$) PEO aqueous solution, a layer of PEO coils is confined in the space between PVA gel and glass surface, in which the PEO concentration is much higher than that of bulk solution for very long PEO (PEO 4E6). When the actual PEO concentration in the confined space is lower than the overlap concentration, PEO blobs screen the adsorption of PVA blob to glass substrate, and this gives a lower frictional stress than that in pure water in slow sliding region (PEO 2E4 $c/c^* \leq 1$, PEO 4E6 $c/c^* = 0.01$). This screening effect is not sensitive to normal pressure. For very long PEO, the chains start to be entangled even when the bulk concentration is in the dilute region (PEO 4E6 $c/c^* > 0.1$). In this case, the adsorption of PVA to the glass substrate is completely screened, and the friction is due to the viscous resistance of the entangled PEO layer. This gives a higher friction than that in pure water at slow sliding region. The shear thinning of the entangled chains in the confined space occurs even at the lowest sliding velocity of the present study to give a "plateau" region of friction. At fast sliding velocity region ($v > 0.01$ m/s), after the "plateau", all the friction curves superpose with the curve in pure water. In this velocity region, polymer depletion layer on the glass surface is induced hydrodynamically, and the friction in this region is due to hydrodynamic lubrication of solvent with a viscosity close to that of water.

Acknowledgment. This work is supported by Grant-in-Aid for the Specially Promoted Research from the Ministry of Education, Science, Sports and Culture of Japan.

References and Notes

(1) McCutchen, C. W. *Wear* **1962**, 5, 1.
(2) McCutchen, C. W. *Lubrication of Joints, the Joints and Synovial Fluid*; Academic Press: New York, 1978.
(3) Dowson, D.; Unsworth, A.; Wright, V. *J. Mech. Eng. Sci.* **1970**, *12*, 364.
(4) Ateshian, G. A.; Wang, H. Q.; Lai, W. M. *J. Tribol.* **1998**, *120*, 241.
(5) Hodge, W. A.; Fijian, R. S.; Carlson, K. L.; Burgess, R. G.; Harris, W. H.; Mann, R. W. *Proc. Natl. Acad. Sci. U.S.A.* **1986**, *83*, 2879.
(6) Grodzinsky, A. J. *CRC Crit. Rev. Biomed. Eng.* **1985**, *9*, 133.
(7) Buschmann, M. D.; Grodzinsky, A. J. *J. Biomech. Eng.* **1995**, *117*, 179.
(8) Wojtys, E. M.; Chan, D. B. *Instrum. Course Lect.* **2005**, *54*, 323.
(9) Persson, B. N. J. *Sliding Friction: Physical Principles and Applications*, 2nd ed.; NanoScience and Technology Series; Springer: Berlin, 1998.
(10) Fung, Y. C. *Biomechanics: Mechanical Properties of Living Tissues*, 2nd ed.; Springer-Verlag: New York, 1993.
(11) Gong, J. P.; Higa, M.; Iwasaki, Y.; Katsuyama, Y.; Osada, Y. *J. Phys. Chem. B* **1997**, *101*, 5487.
(12) Gong, J. P.; Osada, Y. *J. Chem. Phys.* **1998**, *109*, 8062.
(13) Gong, J. P.; Iwasaki, Y.; Osada, Y.; Kurihara, K.; Hamai, Y. *J. Phys. Chem. B* **1999**, *103*, 6001.
(14) Gong, J. P.; Kagata, G.; Osada, Y. *J. Phys. Chem. B* **1999**, *103*, 6007.
(15) Gong, J. P.; Iwasaki, Y.; Osada, Y. *J. Phys. Chem. B* **2000**, *104*, 3423.
(16) Gong, J. P.; Kurokawa, T.; Narita, T.; Kagata, K.; Osada, Y.; Nishimura, G.; Kinjo, M. *J. Am. Chem. Soc.* **2001**, *123*, 5582.
(17) Kagata, G.; Gong, J. P.; Osada, Y. *J. Phys. Chem. B* **2002**, *106*, 4596.
(18) Kurokawa, T.; Gong, J. P.; Osada, Y. *Macromolecules* **2002**, *35*, 8161.
(19) Baumberger, T.; Caroli, C.; Ronsin, O. *Phys. Rev. Lett.* **2002**, *88*, 75509.
(20) Kagata, G.; Gong, J. P.; Osada, Y. *J. Phys. Chem. B* **2003**, *107*, 10221.
(21) Baumberger, T.; Caroli, C.; Ronsin, O. *Eur. Phys. J. E* **2003**, *11*, 85.
(22) Ohsedo, Y.; Takashina, R.; Gong, J. P.; Osada, Y. *Langmiur* **2004**, *20*, 6549.
(23) Tada, T.; Kaneko, D.; Gong, J. P.; Kaneko, T.; Osada, Y. *Tribol. Lett.* **2004**, *17*, 505.
(24) Kaneko, D.; Tada, T.; Kurokawa, T.; Gong, J. P.; Osada, Y. *Adv. Mater.* **2004**, *17*, 535.
(25) Kurokawa, T.; Tominaga, T.; Katsuyama, Y.; Kuwabara, R.; Furukawa, H.; Osada, Y.; Gong, J. P. *Langmiur* **2005**, *21*, 8643.
(26) Nitta, Y.; Haga, H.; Kawabata, K. *J. Phys. IV* **2002**, *12*, 319.
(27) Kampf, N.; Raviv, U.; Klein, J. *Macromolecules* **2004**, *37*, 1134.
(28) Chestakova, A.; Lau, W.; Kumacheva, E. *Macromolecules* **2004**, *37*, 5047.
(29) Trieu, H.; Qutubuddin, S. *Polymer* **1995**, *36*, 2531.
(30) de Gennes, P. G. *Scaling Concept in Polymer Physics;* Cornell University Press: Ithaca, NY, 1979.
(31) Teraoka, I. *Polymer Solution*; John Wiley & Sons: New York, 2002; p 64.
(32) Bailey, F. E., Jr.; Koleske, J. V. *Poly(ethylene oxide)*; Academic Press: London, 1976.
(33) Doi, M.; Edward, S. F. *The Theory of Polymer Dynamics;* Claredon Press: Oxford, 1986.
(34) Degre, G.; Joseph, P.; Tabeling, P.; Lerouge, S.; Cloitre, M.; Ajdari, A. *Appl. Phys. Lett.* **2006**, *89*, 024104.
(35) Jendrejack, R. M.; Schwartz, D. C.; de Pablo, J. J.; Graham, M. D. *J. Chem. Phys.* **2004**, *120*, 2513.

MA0702187